1-1-2006

Selective excitation of the LP11 mode in step index fiber using a phase mask

Waleed Mohammed
University of Central Florida

Mahesh Pitchumani
University of Central Florida

Alok Mehta
University of Central Florida

Eric G. Johnson
University of Central Florida

Selective excitation of the LP_{11} mode in step index fiber using a phase mask

Waleed Mohammed
Mahesh Pitchumani
Alok Mehta
Eric G. Johnson, FELLOW SPIE
University of Central Florida
College of Optics and Photonics/CREOL
Orlando, Florida 32816-2700
E-mail: eric@creol.ucf.edu

Abstract. We present a novel mode selective coupling technique for step index fiber. This technique utilizes phase matching for excitation of higher-order modes while suppressing the fundamental mode. Using this technique, a phase element is fabricated and tested to demonstrate the high coupling efficiency to the LP_{11} mode. In addition, we derive an analytical expression of the coupling efficiency of the LP_{11} using a single phase element.
[DOI: 10.1117/1.2219425]

Subject terms: selective excitation; mode coupling; fiber optics; phase matching; fiber coupling.

Paper 050524R received Jun. 30, 2005; revised manuscript received Nov. 28, 2005; accepted for publication Dec. 9, 2005; published online Jul. 26, 2006.

1 Introduction

In many fiber systems, higher-order guided modes have unique optical properties compared to the fundamental mode in terms of their intensity distribution, polarization, and phase properties. Introducing an efficient and selective coupling technique allows one to exploit their unique properties in several applications such as short distance data transmission and mode division multiplexing.[1] Fiber sensing applications also require spreading the power in the cladding region, which can be accomplished though the excitation of higher-order modes.

Several mode selective coupling schemes have been presented based on angular selective coupling[2] or using a tilted grating written in the core of the fiber using holography techniques.[3] On the other hand, Ref. 4 presents a novel diffractive vortex lens to couple the light to higher-order azimuthal modes to avoid the central deformation of the refractive index profile in graded index fibers.

We present an efficient mode selective excitation of the LP_{11} mode in a step index fiber that sustains a few modes by introducing a phase element that tailors the light at the input of the fiber system, in a similar fashion as in Ref. 5 The excitation of this mode is achieved through placing a phase element in the path of the input light as depicted in Fig. 1. The design of this optical component depends on the physical structure of the fiber and on the phase profile of the specific mode that is excited. In this work, we introduce a phase coupling element with a phase profile equivalent to that of the LP_{11} mode. Using this element, we demonstrate that the field at the input facet of the fiber sustains the same phase profile as the LP_{11} mode. On the other hand, its amplitude is different. This difference corresponds to a reduction of the coupling efficiency to this mode during the testing process. However, we have experimentally achieved a selective coupling efficiency as high as 81% when using this element for selective mode excitation to the LP_{11} mode. To verify this result, we derived a closed-form solution for the LP_{11} mode selective coupling efficiency when using this phase element. This analytical solution shows the dependence of the coupling efficiency on the fiber structure and the light source parameters.

2 Theory

For a step index fiber of core radius a and a working wavelength λ, the field distribution of the guided linearly polarized modes can be represented as follows,[6]

$$\psi_{v,m}(r,\theta,z)=\begin{cases} A_{v,m}J_m\left(u_{v,m}\dfrac{r}{a}\right) \\ \times\cos(m\theta)\exp(-i\beta_{v,m}z) \qquad r\leqslant a \\ \\ A_{v,m}\dfrac{J_m(u_{v,m})}{K_m(w_{v,m})}K_m\left(w_{v,m}\dfrac{r}{a}\right) \\ \times\cos(m\theta)\exp(-i\beta_{v,m}z) \qquad r>a \end{cases} . \tag{1}$$

In Eq. (1), the suffixes v and m are the indices for the guided radial and azimuthal components, respectively, and $A_{v,m}$ is the excitation coefficient of the $LP_{v,m}$ mode. It is defined as the square root of the power coupling coefficient $\eta_{v,m}$, represented by the following overlap integral

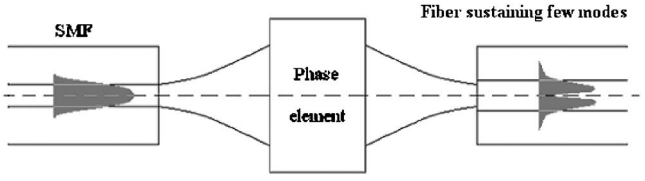

Fig. 1 The main coupling scheme for selective excitation of the LP_{11} mode using a phase element for mode conversion.

0091-3286/2006/$22.00 © 2006 SPIE

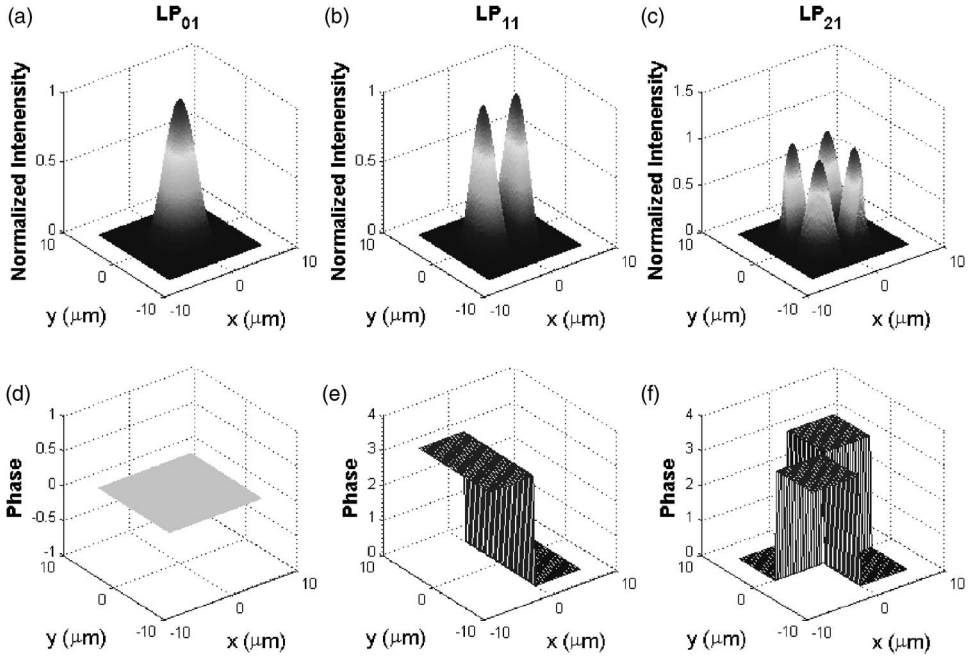

Fig. 2 Intensity distributions of the first three modes: (a) LP_{01}, (b) LP_{11}, (c) LP_{21}, and phase distributions of the first three higher order modes: (a) LP_{01}, (b) LP_{11}, and (c) LP_{21}.

$$\eta_{v,m} = \frac{\left| \int_0^{2\pi} \int_0^{\infty} E_{\text{in}}(r,\theta) \cdot \psi_{v,m}(r,\theta,0)^* r dr d\theta \right|^2}{\int_0^{2\pi} \int_0^{\infty} |E_{\text{in}}(r,\theta)|^2 r dr d\theta \int_0^{2\pi} \int_0^{\infty} |\psi_{v,m}(r,\theta,0)|^2 r dr d\theta}, \quad (2)$$

where $E_{\text{in}}(r,\theta)$ is the field profile at the input facet of the fiber. J_m and K_m are the m'th-order Bessel and modified Bessel functions, respectively, $u_{v,m}$ and $w_{v,m}$ are the normalized transverse propagation constants inside the core, and the cladding, respectively, and $\beta_{v,m}$ is the longitudinal propagation constant. These constants are related through the following formulae

$$u_{v,m} = \beta_{v,m} a,$$

$$V^2 = u_{v,m}^2 + w_{v,m}^2,$$

$$V = \frac{2\pi a}{\lambda} \sqrt{n_{\text{core}}^2 - n_{\text{clad}}^2}, \quad (3)$$

where n_{core} and n_{core} are the core and cladding refractive indices, respectively. In addition, Fig. 2 depicts the amplitude and phase profiles of the first few linearly polarized modes. On closer inspection of the phase profiles of these modes, one notices that they are orthogonal to each other. Thus, to selectively excite one particular mode, it is sufficient to match the phase profile of that specific mode. This can be achieved through phase modulation of the input field by placing a proper phase element in its path, as shown in Fig. 3. In this setup, the first lens collimates the light out of the single mode fiber (SMF), and the second lens focuses the phase modulated light to the input facet of a larger core fiber that sustains more than one mode. We refer to this fiber as a large core fiber. Proper selection of the focal length of the focusing lens has a great impact on achieving high coupling efficiency to the LP_{11}, as we present later in this section.

For the coupling scheme presented in Fig. 3, the light out of the SMF is assumed to be Gaussian with a beam waist defined as[7]

$$w_S = a_S(0.65 + 1.619V_S^{-1.5} + 2.879V_S^{-6}). \quad (4)$$

In Eq. (4), a_S and V_S are the SMF radius and its V-number, respectively. The field immediately after the collimating lens has a beam waist of

$$w_g = w_S \left[1 + \left(\frac{L\lambda}{\pi w_S^2} \right)^2 \right]^{1/2}. \quad (5)$$

Assuming perfect collimation, the beam waist at the phase element will be w_g as well.

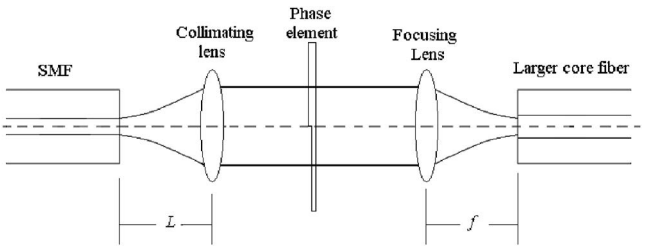

Fig. 3 The coupling scheme showing the phase element placed in the path of the input beam.

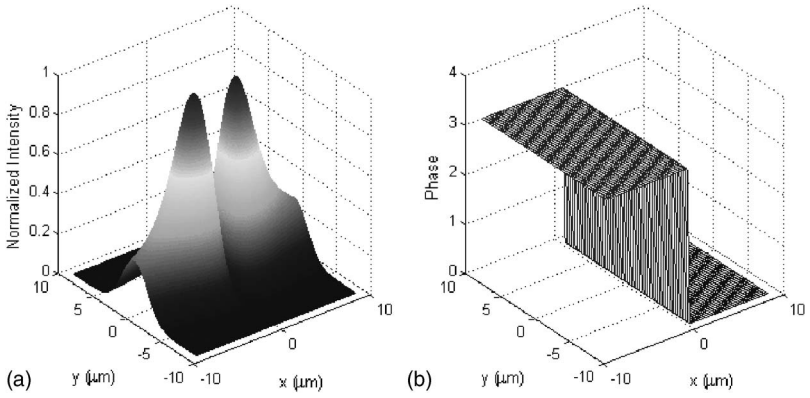

Fig. 4 The calculated (a) amplitude and (b) phase profiles of the field at the input facet of the large core fiber.

The phase coupling element that we introduce has a phase profile identical to that of the LP_{11} mode. The transmittance $T_{(x,y)}$ of this phase element can be represented by a sign function as follows

$$T(x,y) = \mathrm{sign}(x)$$

$$\mathrm{sign}(x) = \begin{cases} 1 & x > 0 \\ 0 & x = 0 \\ -1 & x < 0 \end{cases}. \tag{6}$$

The field distribution at the input of the fiber can be calculated using the Fresnel approximation as follows

$$\begin{aligned} E_{\mathrm{in}}(x,y) &= \frac{i}{\lambda f}\int_{x'=-\infty}^{\infty}\int_{y'=-\infty}^{\infty} \mathrm{sign}(x') \\ &\quad \times \exp\left(-\frac{x'^2+y'^2}{2w_g^2}\right)\exp\left(\frac{-ik}{f}\right)(xx'+yy')dx'dy' \\ &= \frac{2i\pi w_g^2}{\lambda f}\exp\left(-\frac{x^2+y^2}{2w_G^2}\right)\cdot \mathrm{erfi}\left(\frac{x}{\sqrt{2}w_G}\right), \end{aligned} \tag{7}$$

where

$$\mathrm{erfi}(z) = \mathrm{erfi}(iz) = \frac{2i}{\sqrt{\pi}}\int_0^z \exp(t^2)dt, \tag{8}$$

and $w_G = \lambda \cdot f/2\pi w_g$. In Eq. (7), f represents the effective focal length of the second lens in Fig. 3, and k is the wave number of the light $2\pi/\lambda$. The derivation of Eq. (7) is given in the Appendix in Sec. 5. In addition, the input Gaussian beam is assumed, without loss of generality, to be linearly polarized along the x direction. Notice that we used Cartesian coordinates to represent both the phase transmittance of the coupling element and the field at the input of the large core fiber. However, it is more convenient to use polar coordinates in this cylindrical symmetric structure. Defining the following normalized polar coordinates

$$\rho = \left(\frac{x^2+y^2}{2w_G^2}\right)^{1/2}$$

$$\theta = \tan^{-1}(y/x), \tag{9}$$

Eq. (7) can be written as follows

$$E_{\mathrm{in}}(\rho,\theta) = \frac{2i\pi w_g^2}{\lambda f}\exp(-\rho^2)\cdot \mathrm{erfi}(\rho\cos\theta). \tag{10}$$

The amplitude and phase distributions of E_{in} are depicted in Fig. 4. Notice that the phase profile matches that of the LP_{11} mode presented in Fig. 3(e). However, the amplitude differs from that presented in Fig. 3(b). This amplitude mismatch reduces the coupling efficiency to the LP_{11} mode. To estimate the selective coupling efficiency using this phase element, we apply the overlap integral in Eq. (3) after a coordinate change to the normalized polar coordinates defined by Eq. (9). For the LP_{11} mode, the overlap integral can be written as

$$\eta_{v,m} = \frac{|L|^2}{D_1 \cdot D_2}, \tag{11}$$

where

$$\begin{aligned} L = &\int_0^{2\pi}\int_0^{a/\sqrt{2}w_G} \exp(-\rho^2)\cdot \mathrm{erfi}(\rho\cos\theta) \\ &\cdot J_m(b_{11}\rho)\rho d\rho d\theta + \int_0^{2\pi}\int_{a/\sqrt{2}w_G}^{\infty} \exp(\\ &-\rho^2)\cdot \mathrm{erfi}(\rho\cos\theta)\cdot\left[\frac{J_m(u_{11})}{K_m(w_{11})}\right]K_m(c_{11}\rho)\rho d\rho d\theta, \end{aligned} \tag{12}$$

$$D_1 = \frac{\lambda^2 f^2}{2\pi^2 w_g^2}\int_0^{2\pi}\int_0^{\infty} |\exp(-\rho^2)\cdot \mathrm{erfi}(\rho\cos\theta)|^2 \rho d\rho d\theta, \tag{13}$$

and

$$D_2 = \int_0^{2\pi} \int_0^{a/\sqrt{2}w_G} |J_m(b_{11}\rho)|^2 \rho d\rho d\theta + \int_0^{2\pi} \int_{a/\sqrt{2}w_G}^{\infty} \left| \left[\frac{J_m(u_{11})}{K_m(w_{11})} \right] K_m(c_{11}\rho) \right|^2 \rho d\rho d\theta. \quad (14)$$

In Eqs. (11)–(14), b_{11} and c_{11} are defined as

$$b_{11} = \frac{u_{11}\sqrt{2}w_G}{a},$$

$$c_{11} = \frac{w_{11}\sqrt{2}w_G}{a}. \quad (15)$$

Equation (12) can be simplified by expanding the error function in a polynomial series around zero as

$$\mathrm{erfi}(z) = \frac{2}{\sqrt{\pi}} \sum_{n=0}^{\infty} \frac{(z)^{2n+1}}{n!(2n+1)}. \quad (16)$$

Using this expansion, Eq. (12) can be written as,

$$L = \frac{2}{\sqrt{\pi}} \sum_{n=0}^{\infty} \frac{1}{n!(2n+1)} \int_0^{2\pi} (\cos\theta)^{2n+1} d\theta \times \left[\int_0^{\infty} \exp[-(\rho^2)] \cdot \psi_{11}(\rho) \rho^{2n+2} d\rho \right], \quad (17)$$

where $\psi_{11}(\rho)$ is the LP_{11} mode radial dependant term defined as

$$\psi_{11}(\rho) = \begin{cases} J_1(b_{11}\rho) & \rho \leq a/\sqrt{2}w_G \\ \left[\frac{J_1(u_{11})}{K_1(w_{11})} \right] K_1(c_{11}\rho) & \rho > a/\sqrt{2}w_G \end{cases}. \quad (18)$$

To obtain a closed-form solution of the integral in Eq. (17), $\psi_{11}(\rho)$ is approximated by a first-order Hermite-Gaussian as follows[8]

$$\psi_{11}(\rho) \approx p_1 \rho \exp[-(p_2\rho^2)], \quad (19)$$

where p_1 and p_2 are constants. The values of these constants can be obtained by applying two constraints. First, the area under both curves is equal,

$$\int_0^{\infty} \psi_{11}(\rho)\rho d\rho = \int_0^{\infty} p_1 \rho \exp[-(p_2\rho^2)]\rho d\rho. \quad (20)$$

Applying this constraint, we obtain the following linear relation between the two constants

$$p_1 = hp_2$$

$$h = 2\left\{ \frac{[1 - J_0(u_{11})]}{b_{11}} + \left[\frac{J_1(u_{11})}{K_1(w_{11})} \right] \frac{K_0(w_{11})}{c_{11}} \right\}. \quad (21)$$

In the second constraint, the value of p_2 is obtained by minimizing the profile amplitude error δR, defined as

$$\delta R = \psi_{11}(\rho) - hp_2\rho \exp(-p_2\rho^2). \quad (22)$$

Using these approximations, Eq. (14) can be further simplified as

$$L = p_1^2 \left| \sum_{n=0}^{\infty} \frac{\sqrt{\pi}(n+1)(2n)!}{2^n n!} (p_2+1)^{-(1+n)} \right|^2. \quad (23)$$

In the denominator, the first integral D_1 is very difficult to be solved analytically. However, neglecting the Fresnel losses from the phase element and the lens, we can apply Parseval's theory, since E_{in} is proportional to the Fourier transform of the input Gaussian beam phase modulated by the coupling element. Thus,

$$D_1 = \frac{\pi w_g^2}{\lambda^2 f^2}. \quad (24)$$

The second integral in the denominator part of Eq. (11) has the following solution

$$D_2 = \pi a^2 H(u_{11}, w_{11}), \quad (25)$$

where

$$H(u_{11}, w_{11}) = [J_1^2(u_{11}) - J_0(u_{11})J_2(u_{11})] + \left[\frac{J_1(u_{11})}{K_1(w_{11})} \right] \times [K_0(w_{11})K_2(w_{11}) - K_1^2(w_{11})]. \quad (26)$$

Substituting Eqs. (23)–(25) into Eq. (11), we obtain the following expression for the coupling efficiency

$$\eta_{11} = \frac{\lambda^2 f^2 p_1^2 \left| \sum_{n=0}^{\infty} \frac{\sqrt{\pi}(n+1)2n!}{2^n n!} (p_2+1)^{-(1+n)} \right|^2}{\pi^2 w_g^2 a^2 H(u_{11}, w_{11})}. \quad (27)$$

This expression is represented in terms of an infinite series. However, a few expansion terms might only be needed to obtain a precise value of η_{11}. Figure 5(a) depicts the coupling efficiency as a function of the number of expansion terms. In these calculations, we consider an effective focal length f of 8 mm for the focusing lens. The figure shows that by including more than 16 expansion terms into the efficiency calculation, the calculated value of η_{11} converges to a stable value. Therefore, in the rest of this work we use 16 expansion terms to evaluate η_{11} when using the expression in Eq. (27). To predict the accuracy of this expression, we compare the exact numerical calculation of the overlap integral in Eqs. (2) and (27) as a function of f. These results are depicted in Fig. 5(b). In the numerical calculations, E_{in} is computed by using the Fresnel propagation of the input Gaussian beam phase modulated by the coupling element through the second lens. The figure shows a great correspondence between both cases. However, the slight difference in the graphs is mainly due to the first-order Hermite-Gaussian approximation, as presented in Eq. (19). Additionally, the graphs show that the coupling efficiency is maximized around $f=8$ mm. This seems contradictory with Eq. (27) due to the presence of f^2 in the numerator. The explanation for the maximization of η_{11} at a specific effective focal length value can be traced to the formulation

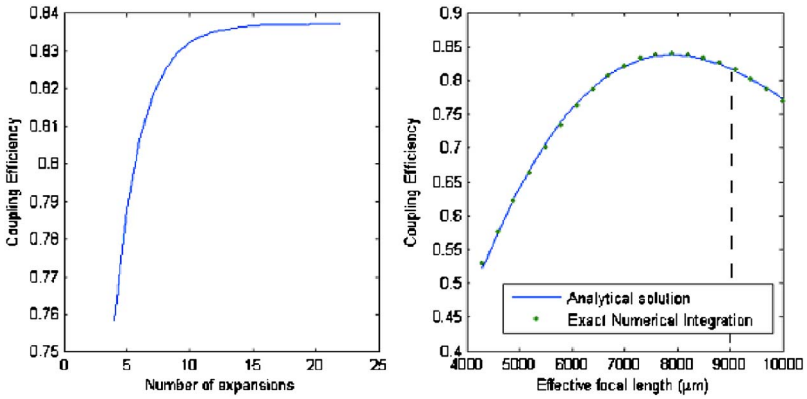

Fig. 5 The coupling efficiency at a focal length of 8 mm as a function of the number of expansions. b The calculated coupling efficiencies to the LP_{11} mode using the analytical form in Eq. (12) using 16 expansion terms and the exact numerical integration.

of p_1 and p_2. However, constants p_1 and p_2 implicitly depend on f through b_{11}, c_{11}, and w_g, as presented in Eqs. (15) and (21). Figure 6 shows the values of p_1 and p_2 as a function of f. Notice that both p_1 and p_2 increases with f.

3 Experimental Results

In our experimental setup, a HeNe laser source is coupled to a single mode fiber and the output is then collimated using a 20× objective lens. The phase modulated light is then coupled into a larger core fiber that sustains a few modes using a 20× objective lens with effective focal length of 9 mm. The fiber used is a Corning SMF 28, which has a single mode at 1550 nm, and supports four modes at a wavelength of 632.8 nm. Without any phase elements, we maximized the light coupled to the LP_{01} to guarantee minimum tilt and shift in the input beam. The phase element shown in Fig. 7(a) was fabricated in Shiply PR1805 photoresist using a stepper system. The refractive index of the photoresist is 1.6406 at the working wavelength. To achieve a π phase shift, the step height was set to 494 nm. Using this element, the resulting far-field intensity distribution at the output of the fiber is depicted in Fig. 7(b). The figure shows that the light is selectively coupled to the LP_{11} mode. Measuring the output power, 81.4% of the power at the input facet of the large core fiber is coupled to the LP_{11} mode. This value is very close to the calculated coupling efficiency of 83.7% using Eq. (27), shown as the dashed line in Fig. 5(b). The cross talk is minimized by properly aligning the input light and the phase element to be on axis with the few-modes fiber.

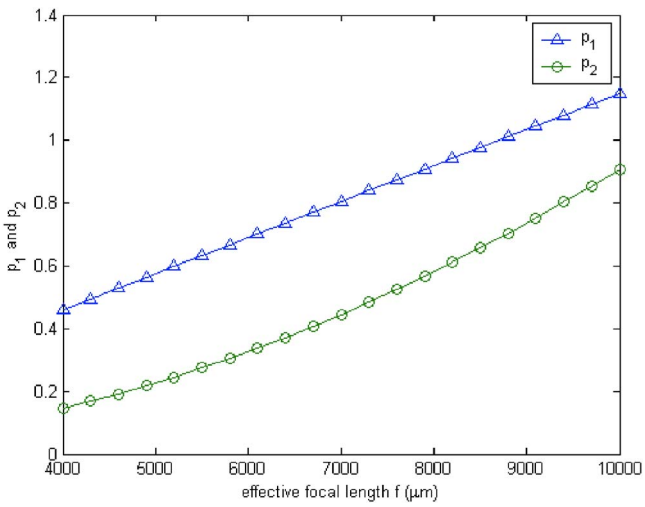

Fig. 6 Dependence on values of p_1 and p_2 on effective focal length showing increasing relationship for both parameters.

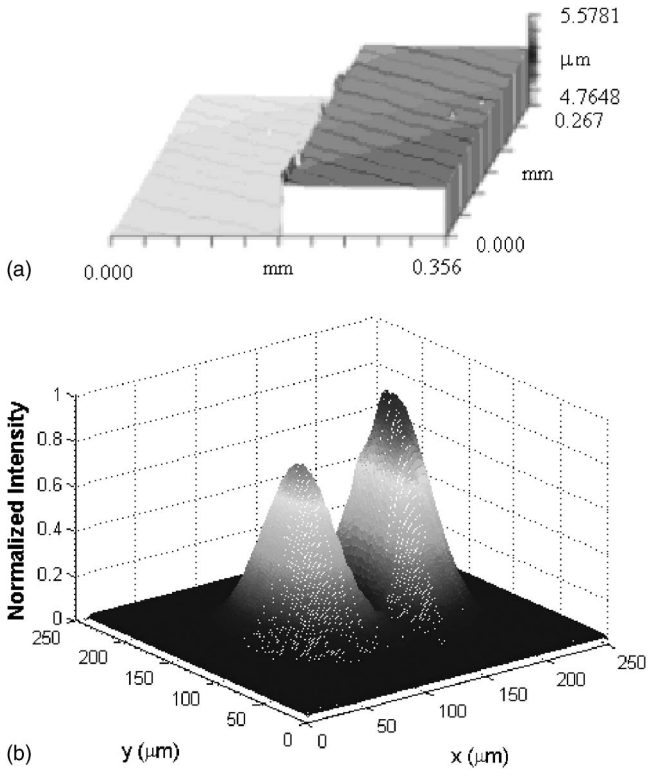

Fig. 7 Zygo image of the phase element for coupling to the LP_{11} mode fabricated in PR1805 photoresist. (b) Observed far-field intensity distributions of the light at the out of the fiber using this phase element.

4 Conclusion

We theoretically and experimentally investigate a mode selective coupling scheme based on phase matching. Using a phase element where the phase profile matches the LP_{11} mode, an experimentally measured selective coupling efficiency as high as 81% is obtained. In addition, we derive a closed-form solution of the coupling efficiency using series expansion of the imaginary error function and approximating the radial dependent term by a Hermite-Gaussian of the first order. Theoretically, results obtained using this analytical solution are seen to coincide with the exact numerical integration for the coupling efficiency. Additionally, the measured coupling efficiency matches to a great extent the predicted one obtained from the analytical solution. However, to achieve high-mode selectivity coupling, a precise alignment is required. To further improve the coupling efficiencies, dual elements have to be used to match both phase and amplitude of the desired modes, which is currently being investigated.

5 Appendix

The field distribution at the input facet of the fiber is defined as

$$E_{\text{in}}(x,y) = \frac{i}{\lambda f}\int_{x'=-\infty}^{\infty}\int_{y'=-\infty}^{\infty} \text{sign}(x') \times \exp\left(-\frac{x'^2+y'^2}{2w_g^2}\right) \times \exp\left[\frac{-ik}{f}(xx'+yy')dx'dy'\right], \tag{28}$$

$$E_{\text{in}}(x,y) = \frac{i}{\lambda f}\int_{x'=-\infty}^{\infty}\int_{y'=-\infty}^{\infty} \text{sign}(x') \times \exp\left(-\frac{x'^2+y'^2}{2w_g^2}\right) \times \exp\left[\frac{-ik}{f}(xx'+yy')dx'dy'\right]. \tag{29}$$

Separating the two integrals in x and y,

$$E_{\text{in}}(x,y) = \frac{i}{\lambda f}\left[\int_{-\infty}^{\infty} \text{sign}(x')\exp\left(\frac{-x'^2}{2w_g^2} - \frac{ikx}{f}x'\right)dx'\right] \cdot \left[\int_{-\infty}^{\infty} \exp\left(\frac{-y'^2}{2w_g^2} - \frac{iky}{f}y'\right)dy'\right]. \tag{30}$$

The integration over y has a straightforward Gaussian solution; however, the integration over x is expanded into two integrations around zero as follows

$$E_{\text{in}}(x,y) = \frac{i}{\lambda f}\left[\int_0^{\infty} \exp\left(\frac{-x'^2}{2w_g^2} - \frac{ikx}{f}x'\right)dx' - \int_{-\infty}^{0} \exp\left(\frac{-x'^2}{2w_g^2} - \frac{ikx}{f}x'\right)dx'\right] \times \left[w_g\sqrt{2\pi}\cdot\exp\left(-\frac{k^2\cdot w_g^2\cdot y^2}{2\cdot f^2}\right)\right]. \tag{31}$$

The integration over x can be further simplified by completing the squares in the exponents as following

$$\left(\exp\left(-\frac{k^2\cdot w_g^2\cdot x^2}{2\cdot f^2}\right)\left\{\int_0^{\infty}\exp\left[-\frac{1}{w_g^2}\cdot\left(x'-\frac{iw_g^2kx}{f}\right)^2\right]dx' - \int_{-\infty}^{0}\exp\left[-\frac{1}{w_g^2}\cdot\left(x'-\frac{iw_g^2kx}{f}\right)^2\right]dx'\right\}\right). \tag{32}$$

Defining the following variables

$$\bar{x} = \frac{\frac{x'}{w_g} - \frac{iw_gkx}{f}}{i\sqrt{2}}$$

for the first integral and

$$\bar{x} = -\frac{\frac{x'}{w_g} - \frac{iw_gkx}{f}}{i\sqrt{2}}$$

for the second integral, the previous formula is simplified to

$$\left\{\frac{iw_g}{\sqrt{2}}\exp\left(-\frac{k^2\cdot w_g^2\cdot x^2}{2\cdot f^2}\right)\left[\int_{-\frac{w_gkx}{f\sqrt{2}}}^{\infty}\exp(\bar{x}^2)d\bar{x} - \int_{\frac{w_gkx}{f\sqrt{2}}}^{\infty}\exp(\bar{x}^2)d\bar{x}\right]\right\}. \tag{33}$$

The two integral subtraction can be simplified into one integral by changing the integral limits as follows

$$\left[\frac{iw_g}{\sqrt{2}}\exp\left(-\frac{k^2\cdot w_g^2\cdot x^2}{2\cdot f^2}\right)\int_{-\frac{w_gkx}{f\sqrt{2}}}^{\frac{w_gkx}{f\sqrt{2}}}\exp(\bar{x}^2)d\bar{x}\right]. \tag{34}$$

The function inside the integral is even, thus the previous integral can be simplified to

$$\left[i2w_g\sqrt{2}\exp\left(-\frac{k^2\cdot w_g^2\cdot x^2}{2\cdot f^2}\right)\int_0^{\frac{w_gkx}{f\sqrt{2}}}\exp(\bar{x}^2)d\bar{x}\right]. \tag{35}$$

Defining a new constant,

$$w_G = \frac{f}{kw_g} = \frac{\lambda f}{2\pi w_g},$$

the total field expression can be written as

$$E_{\text{in}}(x,y) = \frac{-2\sqrt{2}w_g^2\sqrt{2\pi}}{\lambda f}\exp\left(-\frac{y^2+x^2}{2\,.\,w_G^2}\right)\int_0^{x/\sqrt{2}w_G}\exp(\bar{x}^2)d\bar{x}. \tag{36}$$

Defining

$$\text{erfi}(z) = \text{erf}(iz) = \frac{2i}{\sqrt{\pi}}\int_0^z \exp(t^2)dt,$$

then

$$E_{\text{in}}(x,y) = \frac{2i\pi\cdot w_g^2}{\lambda f}\cdot\exp\left(-\frac{y^2+x^2}{2\cdot w_G^2}\right)\text{erfi}\left(\frac{x}{\sqrt{2}\cdot w_G}\right). \tag{37}$$

References

1. R. D. Pechstedt, P. S. J. Russell, T. A. Birks, and F. D. Lloyed-Lucas, "Selective coupling of fiber modes with use of surface-guided Bloch modes supported by dielectric multilayer stacks," *J. Opt. Soc. Am. A* **12**(12), 2655-2659 (1995).
2. M. K. Barnoski and R. J. Marrison, "Angle selective fiber couple," *Appl. Opt.* **15**(1), 253–255 (1976).
3. K. S. Lee and T. Erdogan, "Fiber mode conversion with tilted gratings in an optical fiber," *J. Opt. Soc. Am. A* **18**(5), 1176–1185 (2001).
4. E. G. Johnson, J. Stack, and C. Koehler, "Light coupling by a vortex lens into graded index fiber," *J. Lightwave Technol.* **19**(5), 753–758 (2001).
5. W. Q. Thornburg, B. J. Corrado, and X. D. Zhu, "Selective launching of higher-order modes into an optical fiber with an optical phase shifter," *Opt. Lett.* **19**(7), 454–456 (1994).
6. K. Okamoto, *Fundamentals of Optical Waveguides*, Paul L. Kelley, Ivan P. Kaminow, and Govind P. Agrawal, Eds., pp. 60–64, Academic Press, San Diego, CA (2000).
7. D. Marcuse, *Theory of Dielectric Optical Waveguide*, Academic Press, San Diego, CA (1991).
8. T. Hashimoto, T. Saida, R. Kasahara, and I. Ogawa, "Spot-size conversion of guided optical wave with Gaussian approximation," *J. Lightwave Technol.* **21**(10), 2340 (2003).

Biographies and photographs of authors not available.